

MZ-TH/95-09
 FTUV/95-13
 IFIC/95-13
 July 1995

Longitudinal Contribution to the Alignment
 Polarization of Quarks Produced in
 e^+e^- -Annihilation: An $\mathcal{O}(\alpha_s)$ Effect

S. Groote*, J.G. Körner*

Institut für Physik, Johannes Gutenberg-Universität
 Staudingerweg 7, D-55099 Mainz, Germany.

M.M. Tung**

Departament de Física Teòrica, Universitat de València
 and IFIC, Centre Mixte Universitat València — CSIC,
 C/ Dr. Moliner, 50, E-46100 Burjassot (València), Spain.

ABSTRACT

We calculate the longitudinal contribution to the alignment polarization P^ℓ of quarks produced in e^+e^- annihilation. In the Standard Model, the longitudinal alignment polarization vanishes at the Born term level and thus receives its first non-zero contribution from the $\mathcal{O}(\alpha_s)$ tree graph process. We provide analytical and numerical results for the longitudinal alignment polarization of massless and massive quarks, in particular for the recently discovered top quark.

*Supported in part by the BMFT, FRG, under contracts 06MZ730 and 06MZ566,
 and by HUCAM, EU, under contracts CHRX-CT94-0579

**Feodor-Lynen Fellow

1 Introduction

It is well-known that quarks produced in e^+e^- -annihilation are polarized to a substantial degree. In the absence of beam polarization effects, the polarization of the quarks results from the interplay of the parity-violating and parity-conserving pieces of the Z -exchange and γ -exchange contributions. The degree of polarization of the quarks depends on the type of the produced quarks and their masses, on the c.m. energy (due to the interplay of γ - and Z -exchange contributions), on beam orientation effects, and on beam polarization effects.

Concerning the detectability of the quark's polarization the case of the t -quark is simplest. The top quark is so heavy that it decays before hadronizing. Thus, the polarization of the top quark can be directly studied through an analysis of its subsequent decay modes [1,2]. In the charm and bottom sector, the quark's polarization is expected to be partially transmitted to the fragmentation product when the c - and b -quarks hadronize to the Λ_c - and Λ_b -baryons, respectively, where the polarization transfer is 100%, at least in the heavy quark limit [3]. The issue of the amount of polarization transfer in the finite mass case is an important and interesting issue by itself [4]. Again, the Λ_c or Λ_b polarizations can be determined by their subsequent decays [5].

Predictions for the polarization at the Born term level have been worked out some time ago [1]. First $O(\alpha_s)$ radiative corrections were presented in Ref. [6] where the average alignment polarization $\langle P^\ell \rangle_{\cos \theta}$ was calculated. The averaging was performed with respect to the cosine of the polar beam orientation angle θ .[†] A surprising outcome of the calculation was that the massless quark limit and the radiative correction calculation do not interchange. The reason is that there is a finite spin-flip contribution from collinear gluon emission that survives even as $m_q \rightarrow 0$ [6,7]. The corresponding

[†] The alignment polarization is defined as the component of the polarization along the line of flight of the particle. It is also frequently referred to as the longitudinal polarization. Here we choose the phrase “alignment polarization” in order to set it apart from the “longitudinal” beam orientation component discussed in this paper.

spin-flip contribution is not present in massless QCD. To put it succinctly, one finds $\text{QCD}(m_q \rightarrow 0) \neq \text{QCD}(m_q = 0)$ in the perturbative sector. Such anomalous spin-flip contributions had already been discussed some time ago, in the context of QED [8].

In this paper, we discuss first results on $O(\alpha_s)$ radiative corrections to orientation-dependent polarization effects. We calculate the $O(\alpha_s)$ corrections to the longitudinal component of the quark's alignment polarization. The longitudinal alignment polarization is of particular interest since it vanishes at the Born term level in the Standard Model (SM) due to the fact that the axial-vector current is a first class current in the SM. Directly connected to this observation is the statement that there is no anomalous spin-flip contribution to the longitudinal alignment polarization for vanishing quark masses.

The plan of the paper is as follows. In Sec. 2, we give general expressions for the polar angle dependence of the alignment polarization of quarks produced in e^+e^- -annihilation. The polarization is written in terms of polarized and unpolarized helicity structure functions. In Sec. 3, we list the Born term contributions to the helicity structure functions. Sec. 3 also contains complete results on the one-loop radiative corrections to the alignment polarization in the case $m_q = 0$. These are particularly simple for the longitudinal alignment polarization. We briefly touch on the role of anomalous $O(\alpha_s)$ spin-flip contributions to the alignment polarization. Sec. 4 constitutes the main part of the paper and gives analytical and numerical results on the massive $O(\alpha_s)$ corrections to the longitudinal alignment polarization. We present results on the single and double differential distributions of the polarized longitudinal structure function as well as on its totally integrated form. The Appendix contains our analytical results on the fully integrated structure functions, where we also outline how these closed form expressions were arrived at.

2 Orientation dependence of alignment polarization

In the absence of beam polarization effects, the orientation-dependent alignment polarization is given by (see e.g. [9])

$$P^\ell(\cos \theta) = \frac{d\sigma^\ell/d \cos \theta}{d\sigma/d \cos \theta} = \frac{N^\ell(\cos \theta)}{D(\cos \theta)}, \quad (1)$$

where $d\sigma^\ell$ and $d\sigma$ are the polarized and unpolarized differential production rates, resp., and where

$$N^\ell = \frac{3}{8}(1 + \cos^2 \theta)g_{14}H_U^{4(-)} + \frac{3}{4}\sin^2 \theta g_{14}H_L^{4(-)} + \frac{3}{4}\cos \theta(g_{41}H_F^{1(-)} + g_{42}H_F^{2(-)}), \quad (2)$$

$$\begin{aligned} D = & \frac{3}{8}(1 + \cos^2 \theta)(g_{11}H_U^{1(+)} + g_{12}H_U^{2(+)} \\ & + \frac{3}{4}\sin^2 \theta(g_{11}H_L^{1(+)} + g_{12}H_L^{2(+)})) + \frac{3}{4}\cos \theta g_{44}H_F^{4(+)} \end{aligned} \quad (3)$$

The polar angle θ defines the polar orientation of the electron beam relative to the quark's line of flight. We have defined the sum and the difference of the hadronic tensor with $\lambda_q = \pm \frac{1}{2}$ helicities of the produced quark as

$$H_{\mu\nu}^{(\pm)} = H_{\mu\nu}(\lambda_q = +\frac{1}{2}) \pm H_{\mu\nu}(\lambda_q = -\frac{1}{2}), \quad (4)$$

where the covariant hadronic tensor is defined as usual by

$$H_{\mu\nu} = \sum_{\bar{q}(g) \text{ spins}} \langle q \bar{q}(g) | j_\mu | 0 \rangle \langle 0 | j_\nu^\dagger | q \bar{q}(g) \rangle. \quad (5)$$

The spin sum in Eq. (5) does not include the spin of the quark which one wants to observe. Thus, in the case of two-body production $e^+e^- \rightarrow q\bar{q}$, the hadronic tensor is a function of q^2 and the spin vector s of the quark. For the three-body final state in $e^+e^- \rightarrow q\bar{q}g$, the hadron tensor depends in addition on two Dalitz-plot type variables which will be specified later on. In the three-body case, the hadron tensor has more structure than indicated in Eqs. (2) and (3) which, however, disappears after azimuthal averaging as is always implied in this paper.

In order to exhibit the orientation-dependence of the produced quark, we have projected onto the helicity structure functions $H_U = H_{++} + H_{--}$, $H_L = H_{00}$ and $H_F = H_{++} - H_{--}$, where

$$H_{\lambda_{Z,\gamma}\lambda_{Z,\gamma}} = \varepsilon^\mu(\lambda_{Z,\gamma}) H_{\mu\nu} \varepsilon^{\nu*}(\lambda_{Z,\gamma}), \quad (6)$$

and $\lambda_{Z,\gamma}$ is the helicity of the current or the gauge boson. The hadron tensor $H_{\mu\nu}^i$ carries an extra index i (which is sometimes suppressed) to specify its vector/axial-vector decomposition according to

$$\begin{aligned} H_{\mu\nu}^1 &= \frac{1}{2}(H_{\mu\nu}^{VV} + H_{\mu\nu}^{AA}), \\ H_{\mu\nu}^2 &= \frac{1}{2}(H_{\mu\nu}^{VV} - H_{\mu\nu}^{AA}), \\ H_{\mu\nu}^4 &= \frac{1}{2}(H_{\mu\nu}^{VA} + H_{\mu\nu}^{AV}). \end{aligned} \quad (7)$$

Note that one has $H_{\mu\nu}^{VA} = H_{\mu\nu}^{AV}$ for the unpolarized and alignment polarization cases that are relevant for our discussion.

The electroweak coupling factors, finally, are contained in the coefficients $g_{ij}(s)$. They are given by

$$\begin{aligned}
g_{11} &= Q_f^2 - 2Q_f v_e v_f \text{Re}\chi_Z + (v_e^2 + a_e^2)(v_f^2 + a_f^2)|\chi_Z|^2, \\
g_{12} &= Q_f^2 - 2Q_f v_e v_f \text{Re}\chi_Z + (v_e^2 + a_e^2)(v_f^2 - a_f^2)|\chi_Z|^2, \\
g_{14} &= 2Q_f v_e a_f \text{Re}\chi_Z - (v_e^2 + a_e^2)2v_f a_f |\chi_Z|^2, \\
g_{41} &= 2Q_f a_e v_f \text{Re}\chi_Z - 2v_e a_e (v_f^2 + a_f^2)|\chi_Z|^2, \\
g_{42} &= 2Q_f a_e v_f \text{Re}\chi_Z - 2v_e a_e (v_f^2 - a_f^2)|\chi_Z|^2, \\
g_{44} &= -2Q_f a_e a_f \text{Re}\chi_Z + 4v_e a_e v_f a_f |\chi_Z|^2,
\end{aligned} \tag{8}$$

with the usual notation [9]

$$\begin{aligned}
\chi_Z(s) &= \frac{g M_Z^2 s}{s - M_Z^2 + i M_Z \Gamma_Z}, \quad g = \frac{G_F}{8\sqrt{2}\pi\alpha} \approx 4.49 \cdot 10^{-5} \text{GeV}^{-2}, \\
v_e &= -1 + 4 \sin^2 \theta_W, \quad a_e = -1 \quad \text{for leptons}, \\
v_f &= 1 - \frac{8}{3} \sin^2 \theta_W, \quad a_f = 1 \quad \text{for up-type quarks } (Q_f = \frac{2}{3}), \text{ and} \\
v_f &= -1 + \frac{4}{3} \sin^2 \theta_W, \quad a_f = -1 \quad \text{for down-type quarks } (Q_f = -\frac{1}{3}).
\end{aligned} \tag{9}$$

The average alignment polarization of the quark can be obtained from Eq. (1) by averaging over $\cos\theta$. One has

$$\langle P^\ell(\cos\theta) \rangle = \frac{g_{14} H_{U+L}^{4(-)}}{g_{11} H_{U+L}^{1(+)} + g_{12} H_{U+L}^{2(+)}} =: P_{U+L}^\ell, \tag{11}$$

where we have written $H_{U+L} = H_U + H_L$. In order to project out a given helicity structure function from Eq. (1), one needs to take moment averages of $P^\ell(\cos\theta)$. In our later discussion, we shall be mainly interested in the longitudinal alignment structure function $H_L^{4(-)}$, which can be obtained with respect to the moment factor $(2 - 5 \cos^2 \theta)$. One has

$$\langle (2 - 5 \cos^2 \theta) P^\ell(\cos\theta) \rangle = \frac{g_{14} H_L^{4(-)}}{g_{11} H_{U+L}^{1(+)} + g_{12} H_{U+L}^{2(+)}} =: P_L^\ell. \tag{12}$$

It is important to realize that both the total alignment polarization P_{U+L}^ℓ and the longitudinal alignment polarization P_L^ℓ cover the range $-1 \leq P_L^\ell \leq 1$, since P_{U+L}^ℓ can be

written as a ratio $(a - b)/(a + b)$ and P_L^ℓ as a ratio $(a - b)/(a + b + c)$, where a , b and c are transitions probabilities into definite helicity states and are thus positive definite.

We want to mention that there is a certain amount of simplification of Eq. (1) in the mass-zero limit, where $H^{VV} = H^{AA}$. In this case, $P^\ell(\cos \theta)$ is given by

$$P^\ell(\cos \theta) = \frac{g_{14} \left\{ \frac{3}{8}(1 + \cos^2 \theta)H_U^{4(-)} + \frac{3}{4}\sin^2 \theta H_L^{4(-)} \right\} + \frac{3}{4}\cos \theta g_{41} H_F^{1(-)}}{g_{11} \left\{ \frac{3}{8}(1 + \cos^2 \theta)H_U^{1(+)} + \frac{3}{4}\sin^2 \theta H_L^{1(+)} \right\} + \frac{3}{4}\cos \theta g_{44} H_F^{4(+)}}. \quad (13)$$

3 Born term contribution and the $O(\alpha_s)$ mass-zero case

The Born term contributions to the various hadron tensor components can be easily worked out. If $v = \sqrt{1 - 4m_q^2/q^2}$ denotes the velocity of the quark in the c.m. system, one finds

$$H_U^{4(-)} = 4N_C q^2 v, \quad (14)$$

$$H_L^{4(-)} = 0, \quad (15)$$

$$H_F^{1(-)} = 2N_C q^2(1 + v^2), \quad H_F^{2(-)} = 2N_C q^2(1 - v^2), \quad (16)$$

$$H_U^{1(+)} = 2N_C q^2(1 + v^2), \quad H_U^{2(+)} = 2N_C q^2(1 - v^2) \quad (17)$$

$$H_L^{1(+)} = N_C q^2(1 - v^2) = H_L^{2(+)}, \quad (18)$$

$$H_F^{4(+)} = 4N_C q^2 v, \quad (19)$$

where $N_C = 3$ takes into account that each quark pair occurs in three color states. For the sake of completeness we write down the appropriate two-body $e^+e^- \rightarrow q\bar{q}$ production cross section which reads

$$\frac{d\sigma}{d\cos \theta} = \frac{\pi\alpha^2 v}{3q^4} D(\cos \theta), \quad (20)$$

where the above $H_{U,L}^{1,2(+)}$ and $H_F^{4(+)}$ have to be substituted in the denominator function $D(\cos \theta)$ given in Eq. (3).

The vanishing of the longitudinal alignment component $H_L^{4(-)}$ in Eq. (15) can be understood in many different ways. It is connected with the vanishing of the axial-vector helicity amplitude $H_{0;\lambda_q=\pm\frac{1}{2},\lambda_{\bar{q}}=\pm\frac{1}{2}}^A$, or, alternatively, with the vanishing of the longitudinal

projection of the axial-vector current matrix element, i.e. $(p_1 - p_2)^\mu \bar{u}(p_1) \gamma_\mu \gamma_5 v(p_2) = 0$. In partial wave language, $H_{0;\pm\frac{1}{2},\pm\frac{1}{2}}^A$ is contributed to by the LS -amplitude $L = 1$ and $S = 0$ ($L = 1, S = 1$ does not couple, because the corresponding Clebsch-Gordan coefficient $(LL_zSS_z|J^{\gamma,Z}J_z^{\gamma,Z}) = (1010|10)$ vanishes). However, as is well known from positronium and quarkonium considerations, the charge conjugation quantum number of the $L = 1, S = 0$ state is $C = (-1)^{L+S} = -1$ and thus does not match up with the charge conjugation $C = +1$ of the axial-vector current. Put in a different language, the Born term contribution to the longitudinal alignment polarization is a second class current effect and is thus zero in the SM. The above argument easily generalizes to the n -loop case, where one similarly concludes that its contributions to the longitudinal alignment polarization vanishes. Nonvanishing contributions start coming in from three- or more-body final states as for example from the one-gluon emission graph that will be discussed further on.

Returning to Eq. (1), one can then calculate the Born term contribution to $P^\ell(\cos \theta)$.

On the Z -peak the polarization is ($r_e = 2v_e a_e / (v_e^2 + a_e^2)$)

$$P^\ell(\cos \theta) = -2 \frac{v_f a_f v (1 + \cos^2 \theta) + r_e (v_f^2 + a_f^2 v^2) \cos \theta}{(v_f^2 + a_f^2 v^2) (1 + \cos^2 \theta) + v_f^2 (1 - v^2) \sin^2 \theta + 4r_e v_f a_f v \cos \theta}. \quad (21)$$

The result Eq. (21) agrees with the value of $P^\ell(\cos \theta)$ quoted in Ref. [1]. Note again the absence of the longitudinal contribution proportional to $\sin^2 \theta$ in the numerator. The mass-zero case is easily obtained by setting $v = 1$ in Eq. (21). One can then directly calculate the following SM values for the average of the alignment polarization on the Z -peak. The values are $\langle P^\ell(\cos \theta) \rangle_u \approx -69\%$ and $\langle P^\ell(\cos \theta) \rangle_d \approx -94\%$ for up- and down-type quarks, respectively. By using Eq. (21) it is easy to check that there is very little mass and orientation dependence of $P^\ell(\cos \theta)$ on the Z -peak.

To conclude this section, we shall also list the value of the alignment polarization $P^\ell(\cos \theta)$ in the mass-zero case including $\mathcal{O}(\alpha_s)$ radiative corrections. The longitudinal structure functions $H_L^{(\pm)}$ can easily be calculated since they receive only finite contributions from the one-gluon emission graphs. The (y, z) -Dalitz plot distribution of the relevant longitudinal tree graph contribution is [9]

$$H_L^{4(-)}(y, z) = H_L^{1(+)}(y, z) = 64\pi N_C C_F \alpha_s \frac{1 - y - z}{(1 - y)^2} \quad (22)$$

$(y = 1 - 2p_1 \cdot q/q^2, z = 1 - 2p_2 \cdot q/q^2, p_1 = p_q, p_2 = p_{\bar{q}})$. After z -integration over the (y, z) -Dalitz plot with the appropriate 4-dimensional integration measure, one finds a flat y -distribution

$$\frac{1}{16\pi^2}q^2 \int_0^{1-y} dz \frac{1-y-z}{(1-y)^2} = \frac{1}{32\pi^2}q^2. \quad (23)$$

The remaining y -integration in the interval $[0, 1]$ is trivial and the fully integrated contributions to the longitudinal structure functions are then given by [10]

$$H_L^{4(-)} = H_L^{1(+)} = 2N_C C_F \frac{\alpha_s}{\pi} q^2, \quad (24)$$

where as usual $C_F = 4/3$ denotes the Casimir operator in the fundamental representation of the $SU(3)$ color group. The $O(\alpha_s)$ integration for $m_q = 0$ in Eq. (23) is deceptively simple. The corresponding $O(\alpha_s)$ calculation for $m_q \neq 0$ discussed in Sec. 4 turns out to be considerably more complicated.

To calculate the remaining massless unpolarized (U) and forward-backward (F) structure functions, we need to add the loop contributions. Only the sum of the tree- and loop-contributions to H_U and H_F are IR/M finite. Let us simply list the remaining structure functions including the anomalous contributions to the polarized structure functions $H_U^{4(-)}$ and $H_F^{1(-)}$, i.e. the finite $O(\alpha_s)$ anomalous spin flip contributions that remain as $m_q \rightarrow 0$.

$$H_U^{4(-)} = N_C C_F \frac{\alpha_s}{\pi} (1 - [2]) q^2, \quad H_U^{1(+)} = N_C C_F \frac{\alpha_s}{\pi} q^2, \quad (25)$$

$$H_F^{1(-)} = N_C C_F \frac{\alpha_s}{\pi} (0 - [2]) q^2, \quad H_F^{4(+)} = 0. \quad (26)$$

The anomalous spin-flip contributions are listed in the square brackets. The polarized structure function $H_U^{4(-)}$ can be obtained from [6] (where $U + L$ was calculated) and Eq. (24) using the relation $U = (U + L) - L$. The forward-backward structure function $H_F^{4(+)}$ has been calculated in [11] for the massive quark case and in [12] for the mass-zero case. Since the anomalous spin-flip contributions cancel in the *sum* of helicity transitions, the limit $m_q \rightarrow 0$ is smooth for the unpolarized structure functions. On the other hand, since $H_U^{4(-)} = H_U^{1(+)}$ and $H_F^{1(-)} = H_F^{4(+)}$ in massless QCD, the normal (unbracketed) no-flip contributions to the polarized structure functions $H_U^{4(-)}$ and $H_F^{1(-)}$ can immediately be obtained from the respective unpolarized cases. Thus, e.g. the normal no-flip contribution

to $H_F^{1(-)}$ vanishes since $H_F^{4(+)}$ vanishes. The total contribution to $H_F^{1(-)}$ including the anomalous spin-flip term has been calculated in [13]. Finally, as has been emphasized before, there are no $O(\alpha_s)$ anomalous spin-flip contributions to the longitudinal polarized structure function $H_L^{4(-)}$, since these are associated with collinear gluon emission which are absent in $H_L^{4(-)}$ due to the fact that $H_L^{4(-)}$ vanishes at the Born term level.

4 $O(\alpha_s)$ correction to the longitudinal alignment polarization for $m_q \neq 0$

The calculation of the massive $O(\alpha_s)$ corrections to the longitudinal alignment polarization is straightforward but tedious. One first projects out the relevant longitudinal components and then performs the phase-space integration to obtain the longitudinal polarized structure functions. We mention that we define the longitudinal structure functions with respect to the line of flight of the quark.

The relevant normalized covariant longitudinal projector is thus given by

$$\Pi_L^{\mu\nu} = \varepsilon^\mu(0) \varepsilon^{*\nu}(0) = \frac{1}{p_{1z}^2} \left(p_1^\mu - \frac{p_1 \cdot q}{q^2} q^\mu \right) \left(p_1^\nu - \frac{p_1 \cdot q}{q^2} q^\nu \right), \quad (27)$$

where p_1 is the quark's momentum and q denotes the total four-momentum carried by the gauge boson. In terms of the (y, z) -variables, the longitudinal projector takes the form

$$\Pi_L^{\mu\nu} = \frac{4}{q^2 [(1-y)^2 - \xi]} \left\{ p_1^\mu - \frac{1}{2}(1-y) q^\mu \right\} \left\{ p_1^\nu - \frac{1}{2}(1-y) q^\nu \right\}. \quad (28)$$

A straightforward calculation of the $O(\alpha_s)$ tree graph contribution gives

$$\begin{aligned} H_L^{4(-)}(y, z) &= \Pi_L^{\mu\nu} H_{\mu\nu}^{4(-)}(\text{tree}) \\ &= \frac{8\pi\alpha_s N_C C_F}{\{(1-y)^2 - \xi\}^{3/2}} \left[4(2 - 3\xi + \xi^2) - (16 - 8\xi - 3\xi^2)y \right. \\ &\quad + 8(1 + \xi)y^2 - (8 - 10\xi - \xi^2)z + 4(2 + \xi)yz \\ &\quad \left. - 2\xi(1 - \xi) \left(\frac{y}{z} + \frac{z}{y} \right) - \xi(2 - 3\xi) \frac{y^2}{z} + 4\xi \frac{y^3}{z} + \xi^2 \frac{y^3}{z^2} \right]. \end{aligned} \quad (29)$$

for the longitudinal projection of the vector/axial-vector interference part of the polarized hadron tensor. We have used the abbreviation $\xi = 4m_q^2/q^2$. In calculating the squared

matrix element Eq. (29), we have made use of the covariant form of the alignment polarization 4-vector $s_\mu^\ell = \xi^{-\frac{1}{2}} (\sqrt{(1-y)^2 - \xi}, 0, 0, 1-y)$. In the mass-zero limit $\xi \rightarrow 0$, Eq. (29) can be seen to collapse to the mass-zero case Eq. (22). Since there are no IR singularities when integrating $H_L^{4(-)}$, one does not have to introduce a gluon mass as infrared regulator. Note that the denominator factor $\{(1-y)^2 - \xi\}^{3/2}$ in Eq. (29) vanishes at the edge of phase space where $p_{1z} = 0$ ($\hat{y} = 1 - \sqrt{\xi}$, see Fig. 1). This vanishing, however, does not correspond to a true singularity but is canceled by the numerator factor. In fact, $H_L^{4(-)}$ vanishes at $y = 1 - \sqrt{\xi}$. We shall have to return to this point when doing the y -integration later on.

The integration measure for the (y, z) integration appropriate for the integration of the three-body phase-space is given by

$$dPS = \frac{q^2}{16\pi^2 v} dy dz, \quad (30)$$

where the phase-space region is shown in the Dalitz plot in Fig. 1. The boundary functions $z_\pm(y)$ of the phase space integration are listed in the Appendix together with the boundary values y_\pm . Note that the phase-space factor Eq. (30) is given by the ratio of three-body and two-body phase-space factors, since we are giving our results in terms of the two-body structure functions. For definiteness, we list the appropriate three-body production rate, which is given by

$$\frac{d\sigma}{dy dz d\cos\theta} = \frac{\alpha^2}{48\pi q^2} D(y, z, \cos\theta) \quad (31)$$

where the denominator function Eq. (3) is now written in terms of the (y, z) -dependent three-body structure functions $H_{U,L,F}^{(+)}(y, z)$.

As a first step, we perform the z -integration to obtain the differential y -distribution of the polarized longitudinal structure function $H_L^{4(-)}(y)$. One finds

$$\begin{aligned} H_L^{4(-)}(y) &= \frac{q^2}{16\pi^2 v} \int_{z_-(y)}^{z_+(y)} dz H_L^{4(-)}(y, z) \\ &= \frac{\alpha_s N_C C_F q^2 y}{2\pi v \{(1-y)^2 - \xi\}^{3/2}} \left[-\xi \left\{ 2(1-\xi) + (2-3\xi)y - 4y^2 \right\} \ln \left(\frac{z_+(y)}{z_-(y)} \right) \right. \\ &\quad \left. + \left\{ \frac{(4-\xi)^2(2-\xi)}{2(4y+\xi)} - \frac{1}{2}(16-6\xi-\xi^2) + 2(2+5\xi)y \right\} \sqrt{(1-y)^2 - \xi} \right]. \end{aligned} \quad (32)$$

The vanishing of $H_L^{4(-)}$ at the soft photon point $y = 0$ is explicit in Eq. (32). Also, as mentioned before, $H_L^{4(-)}$ does not become singular at $y_{\max} = 1 - \sqrt{\xi}$, but vanishes at this

point. For $\xi = 0$, one recovers the massless result Eq. (24).

As a next step, we do the y -integration. As just mentioned, Eq. (32) is well-behaved for $y \rightarrow 1 - \sqrt{\xi}$, since the denominator zero is canceled by the numerator factor. However, when integrating Eq. (32) term by term, one does encounter spurious singularities in intermediate steps of the calculation. These spurious singularities will be regularized by slightly deforming the phase-space edge from $y_+ = 1 - \sqrt{\xi}$ to $y_+ = 1 - \sqrt{\xi} - \varepsilon$ (see Fig. 1). The spurious divergences must and do cancel out after all terms are recombined. A complete list of analytical expressions for the necessary spin-dependent integrals encountered in the integration of Eq. (32) is given in the Appendix. Finally, the totally polarized longitudinal structure function is given by

$$\begin{aligned} H_L^{4(-)} &= \int dPS H_L^{4(-)}(y, z) = \int dy H_L^{4(-)}(y) \\ &= \frac{\alpha_s N_C C_F q^2}{2\pi v} \left[4(1 - \xi)(2 - \xi)T_1 - (16 - 8\xi - 3\xi^2)T_2 + 8(1 + \xi)T_3 \right. \\ &\quad \left. - (8 - 10\xi - \xi^2)T_4 + 4(2 + \xi)T_5 - 2\xi(1 - \xi)(T_6 + T_7) \right. \\ &\quad \left. - \xi(2 - 3\xi)T_8 + 4\xi T_9 + \xi^2 T_{10} \right], \end{aligned} \quad (33)$$

where the spurious $\ln \varepsilon$ singularities can be seen to cancel in Eq. (33). Taking the $m_q \rightarrow 0$ limit in Eq. (33) requires some care, but one can check that Eq. (33) reduces to the massless result Eq. (24) as $m_q \rightarrow 0$.

In Figs. 2, the numerical $O(\alpha_s)$ results of the longitudinal alignment polarization and the total cross section are displayed for $e^+e^- \rightarrow \gamma, Z \rightarrow t\bar{t}$ with a top-quark mass of $m_t(m_t) = 174$ GeV. We have considered the running of the strong coupling [14] by evolving $\alpha_s^{(5)}(M_Z) = 0.123$ within 5 flavor QCD to the heavy-quark threshold and then connecting the threshold value to a theory with 6 active flavors. Evidently, it suffices to use the QCD renormalization group equations up to one-loop order. For the bottom quark case to be discussed next, similar matching conditions relate the couplings of the theory with 5 quarks and an effective theory with only 4 quarks.

The top quark production cross section shown in Fig. 2(a) rises steeply from threshold at 348 GeV and then settles down to its asymptotic $1/q^2$ behaviour. The longitudinal alignment polarization P_L^ℓ shown in Fig. 2(b) is negative and remains quite small at less than 1%. It rises from threshold and has only reached one-third of its asymptotic value

$P_L^\ell \simeq \frac{2g_{14}}{3g_{11}} \frac{\alpha_s}{\pi} (1 + \frac{\alpha_s}{\pi})^{-1} \cong -0.64\%$ (modulo logarithmic effects from the running of the coupling constant) at 1000 GeV. In Fig. 3, we show the y -distribution of the longitudinal alignment polarization for three different q^2 -values. The polarization peaks toward maximal y -values, i.e. the polarization is largest for the lower top quark energies where the production cross section is smallest. Note that the y -distribution of the polarization is defined by the $O(\alpha_s)$ tree graph distribution alone, i.e. the polarization distribution in Fig. 3 is an $O(\alpha_s^0)$ effect, since the QCD coupling factor α_s cancels in the numerator and denominator. This explains the sizable polarization values in Fig. 3 as compared to the total $O(\alpha_s)$ polarization values in Fig. 2(b). Note also that the soft-gluon point $y = 0$ does not require special attention because of the afore-mentioned absence of an IR singularity in the polarized longitudinal structure function. The total rate factor in the denominator for Eq. (1) does become singular for $y \rightarrow 0$ leading to the rapid vanishing of the longitudinal alignment polarization as $y \rightarrow 0$.

The results for bottom-quark production are presented in Figs. 4. On the Z -peak, we find for the longitudinal beam alignment polarization a maximal value of $P_L^\ell = -2.05\%$. In the range from 300 GeV to 1000 GeV, P_L^ℓ decreases slightly from -1.4% to -1.2% . This fall-off is mainly due to the logarithmic fall-off of α_s . If one neglects this effect again, the polarization would increase and reach the asymptotic value $P_L^\ell \approx -1.64\%$. We do not present any y -distributions of the longitudinal alignment polarization for the b -quark case since we have not implemented any collinear cuts in the present calculation. In the absence of such cuts, the y -distribution of the polarization is nominally zero when $m_b \rightarrow 0$ because the denominator in the polarization expression is singular for any value of y in this case, due to the collinear singularity at $z = 0$.

We mention that, in our numerical evaluations, we have made use of the simple Schwinger-type approximations derived in Ref. [15] for the unpolarized cross section, which appear in the denominator of the polarization expression Eq. (11).

Acknowledgements. M.M.T. wishes to thank J. Bernabéu, J. Peñarrocha and A. Pich for stimulating discussions and gratefully acknowledges the support given by the Alexander-von-Humboldt Foundation and the Generalitat Valenciana.

Appendix: $q\bar{q}g$ Phase-Space Integration

The boundaries of the three body phase-space are given by the functions

$$z_{\pm} = \frac{2y}{4y + \xi} \left\{ 1 - y - \frac{1}{2}\xi \pm \sqrt{(1 - y)^2 - \xi} \right\}, \quad (\text{A1})$$

where the extremal values of y are

$$y_- = 0, \quad y_+ = 1 - \sqrt{\xi}. \quad (\text{A2})$$

The boundaries of the three-body phase-space are shown in Fig. 1. One first does the z -integration in the above limits. The result is listed in Eq. (32). As mentioned before, one encounters spurious divergences at the upper boundary $y = y_{\max}$ in individual terms when further integrating Eq. (32) over y . These spurious divergencies are regularized by introducing the cutoff ε . Then the spin-dependent integrals with no logarithms have the form ($n = 0, 1; m = 1, 2$)

$$T(n, m) = \int_0^{1-\sqrt{\xi-\varepsilon}} dy \frac{y^m}{(4y + \xi)^n ((1 - y)^2 - \xi)}. \quad (\text{A3})$$

It is not difficult to see by complete induction that the following relation holds

$$4T(n, m) = T(n - 1, m - 1) - \xi T(n, m - 1). \quad (\text{A4})$$

With a short list of the basic integral solutions, one can then successively construct all the remaining integrals.

The second type of integral needed to integrate Eq. (32) involves the additional factor $\ln[z_+(y)/z_-(y)]/\sqrt{(1 - y)^2 - \xi}$ in the integrand of Eq. (A3) where now $n = 0$ and $m = 1, 2, 3$. Using again an appropriate substitution, all the solutions containing also dilogarithms [16] can be found in a straightforward manner. A complete list of integrals encountered in the spin-dependent calculation is the following:

$$\begin{aligned} T_1 &= \int \frac{dy dz}{\{(1 - y)^2 - \xi\}^{3/2}} \\ &= \frac{2(1 - \sqrt{\xi})}{\sqrt{\xi}(2 - \sqrt{\xi})^2} \left[-\ln \varepsilon + \frac{1}{2} \ln \xi - \ln(1 + \sqrt{\xi}) + \ln(1 - \sqrt{\xi}) + \ln 2 \right] \\ &\quad + \frac{4\xi}{(4 - \xi)^2} \left[\frac{3}{2} \ln \xi - \ln(1 + \sqrt{\xi}) - 2 \ln(2 - \sqrt{\xi}) + \ln 2 \right], \end{aligned} \quad (\text{A5})$$

$$\begin{aligned}
T_2 &= \int \frac{dy dz}{\{(1-y)^2 - \xi\}^{3/2}} y \\
&= \frac{2(1-\sqrt{\xi})^2}{\sqrt{\xi}(2-\sqrt{\xi})^2} \left[-\ln \varepsilon + \frac{1}{2} \ln \xi - \ln(1+\sqrt{\xi}) + \ln(1-\sqrt{\xi}) + \ln 2 \right] \\
&\quad - \frac{\xi^2}{(4-\xi)^2} \left[\frac{3}{2} \ln \xi - \ln(1+\sqrt{\xi}) - 2 \ln(2-\sqrt{\xi}) + \ln 2 \right] + \frac{1}{2} \ln \xi \\
&\quad - \ln(1+\sqrt{\xi}) + \ln 2,
\end{aligned} \tag{A6}$$

$$\begin{aligned}
T_3 &= \int \frac{dy dz}{\{(1-y)^2 - \xi\}^{3/2}} y^2 \\
&= \frac{2(1-\sqrt{\xi})^3}{\sqrt{\xi}(2-\sqrt{\xi})^2} \left[-\ln \varepsilon + \frac{1}{2} \ln \xi - \ln(1+\sqrt{\xi}) + \ln(1-\sqrt{\xi}) + \ln 2 \right] \\
&\quad + \frac{\xi^3}{4(4-\xi)^2} \left[\frac{3}{2} \ln \xi - \ln(1+\sqrt{\xi}) - 2 \ln(2-\sqrt{\xi}) + \ln 2 \right] \\
&\quad + \frac{1}{4}(8-\xi) \left[\frac{1}{2} \ln \xi - \ln(1+\sqrt{\xi}) + \ln 2 \right] + 1 - \sqrt{\xi},
\end{aligned} \tag{A7}$$

$$\begin{aligned}
T_4 &= \int \frac{dy dz}{\{(1-y)^2 - \xi\}^{3/2}} z \\
&= 2 \frac{(1-\sqrt{\xi})^2}{(2-\sqrt{\xi})^3} \left[-\ln \varepsilon + \frac{1}{2} \ln \xi - \ln(1+\sqrt{\xi}) + \ln(1-\sqrt{\xi}) + \ln 2 \right] \\
&\quad + \frac{\xi(32-20\xi-\xi^2)}{2(4-\xi)^3} \left[\frac{3}{2} \ln \xi - \ln(1+\sqrt{\xi}) - 2 \ln(2-\sqrt{\xi}) + \ln 2 \right] \\
&\quad + 2 \frac{\xi(1-\sqrt{\xi})}{(4-\xi)(2-\sqrt{\xi})^2} - \frac{1}{2} \left[\frac{1}{2} \ln \xi - \ln(1+\sqrt{\xi}) + \ln 2 \right],
\end{aligned} \tag{A8}$$

$$\begin{aligned}
T_5 &= \int \frac{dy dz}{\{(1-y)^2 - \xi\}^{3/2}} y z \\
&= 2 \left(\frac{1-\sqrt{\xi}}{2-\sqrt{\xi}} \right)^3 \left[-\ln \varepsilon + \frac{1}{2} \ln \xi - \ln(1+\sqrt{\xi}) + \ln(1-\sqrt{\xi}) + \ln 2 \right] \\
&\quad - \frac{\xi^2(12-7\xi)}{2(4-\xi)^3} \left[\frac{3}{2} \ln \xi - \ln(1+\sqrt{\xi}) - 2 \ln(2-\sqrt{\xi}) + \ln 2 \right]
\end{aligned}$$

$$+\frac{2}{4-\xi} \left[\xi \left(\frac{1-\sqrt{\xi}}{2-\sqrt{\xi}} \right)^2 + \sqrt{\xi} - 1 \right] - \frac{1}{2} \left[\frac{1}{2} \ln \xi - \ln(1+\sqrt{\xi}) + \ln 2 \right], \quad (\text{A9})$$

$$\begin{aligned} T_6 &= \int \frac{dy dz}{\{(1-y)^2 - \xi\}^{3/2}} \frac{y}{z} \\ &= 2 \frac{1-\sqrt{\xi}}{\xi(2-\sqrt{\xi})} \left[-\ln \varepsilon + \frac{1}{2} \ln \xi - \ln(1+\sqrt{\xi}) + \ln(1-\sqrt{\xi}) + \ln 2 + 2 \right] \\ &\quad - \frac{4-3\xi}{\xi(4-\xi)} \left[\frac{3}{2} \ln \xi - \ln(1+\sqrt{\xi}) - 2 \ln(2-\sqrt{\xi}) + \ln 2 \right] \\ &\quad - \frac{1}{\xi} \left[\frac{1}{2} \ln \xi - \ln(1+\sqrt{\xi}) + \ln 2 \right] - \frac{2v}{\xi} \ln \left(\frac{1+v}{1-v} \right), \end{aligned} \quad (\text{A10})$$

$$\begin{aligned} T_7 &= \int \frac{dy dz}{\{(1-y)^2 - \xi\}^{3/2}} \frac{z}{y} \\ &= 2 \frac{1-\sqrt{\xi}}{(2-\sqrt{\xi})^3} \left[-\ln \varepsilon + \frac{1}{2} \ln \xi - \ln(1+\sqrt{\xi}) + \ln(1-\sqrt{\xi}) + \ln 2 \right] \\ &\quad - 4 \frac{8-6\xi-\xi^2}{(4-\xi)^3} \left[\frac{3}{2} \ln \xi - \ln(1+\sqrt{\xi}) - 2 \ln(2-\sqrt{\xi}) + \ln 2 \right] \\ &\quad - 8 \frac{1-\sqrt{\xi}}{(4-\xi)(2-\sqrt{\xi})^2}, \end{aligned} \quad (\text{A11})$$

$$\begin{aligned} T_8 &= \int \frac{dy dz}{\{(1-y)^2 - \xi\}^{3/2}} \frac{y^2}{z} \\ &= 2 \frac{(1-\sqrt{\xi})^2}{\xi(2-\sqrt{\xi})} \left[-\ln \varepsilon + \frac{1}{2} \ln \xi - \ln(1+\sqrt{\xi}) + \ln(1-\sqrt{\xi}) + \ln 2 + 2 \right] \\ &\quad - \frac{4-3\xi+\xi^2}{\xi(4-\xi)} \left[\frac{3}{2} \ln \xi - \ln(1+\sqrt{\xi}) - 2 \ln(2-\sqrt{\xi}) + \ln 2 \right] \\ &\quad + \frac{1+\xi}{\xi} \left[-\frac{1}{2} \ln \xi + \ln(1+\sqrt{\xi}) - \ln 2 \right] - \frac{2v}{\xi} \ln \left(\frac{1+v}{1-v} \right) \\ &\quad + \frac{1}{2} \ln \left(\frac{1+w}{1-w} \right)^2 + \frac{1}{2} \left[\frac{1}{2} \ln \xi - \ln(1+\sqrt{\xi}) + 2 \ln(2+\sqrt{\xi}) - 5 \ln 2 \right] \ln(1-w^2) \\ &\quad + \text{Li}_2 \left(\frac{1+w}{2} \right) + \text{Li}_2 \left(\frac{1-w}{2} \right) - 2 \text{Li}_2 \left(\frac{2\sqrt{\xi}}{2+\sqrt{\xi}} \right) - 2 \text{Li}_2 \left(\frac{2+\sqrt{\xi}}{4} \right) \\ &\quad - \frac{1}{6} \pi^2 + \ln^2 2 + \text{Li}_2 \left(\frac{2\sqrt{\xi}}{(2+\sqrt{\xi})(1+w)} \right) + \text{Li}_2 \left(\frac{2\sqrt{\xi}}{(2+\sqrt{\xi})(1-w)} \right) \end{aligned}$$

$$+ \text{Li}_2 \left((2 + \sqrt{\xi}) \frac{(1+w)}{4} \right) + \text{Li}_2 \left((2 + \sqrt{\xi}) \frac{(1-w)}{4} \right), \quad (\text{A12})$$

$$\begin{aligned}
T_9 &= \int \frac{dy dz}{\{(1-y)^2 - \xi\}^{3/2}} \frac{y^3}{z} \\
&= 2 \frac{(1-\sqrt{\xi})^3}{\xi(2-\sqrt{\xi})} \left[-\ln \varepsilon + \frac{1}{2} \ln \xi - \ln(1+\sqrt{\xi}) + \ln(1-\sqrt{\xi}) + \ln 2 + 2 \right] \\
&\quad - \frac{16 + 20\xi - 12\xi^2 + \xi^3}{4\xi(4-\xi)} \left[\frac{3}{2} \ln \xi - \ln(1+\sqrt{\xi}) - 2 \ln(2-\sqrt{\xi}) + \ln 2 \right] \\
&\quad + \left(2 + \frac{1}{4}\xi + \frac{1}{\xi} \right) \left[-\frac{1}{2} \ln \xi + \ln(1+\sqrt{\xi}) - \ln 2 \right] - \left(4 + \frac{2}{\xi} \right) v \ln \left(\frac{1+v}{1-v} \right) \\
&\quad + \frac{3}{2} \ln \left(\frac{1+w}{1-w} \right)^2 + \frac{3}{2} \left[\frac{1}{2} \ln \xi - \ln(1+\sqrt{\xi}) + 2 \ln(2+\sqrt{\xi}) - 5 \ln 2 \right] \ln(1-w^2) \\
&\quad + 3 \left[\text{Li}_2 \left(\frac{1+w}{2} \right) + \text{Li}_2 \left(\frac{1-w}{2} \right) - 2 \text{Li}_2 \left(\frac{2\sqrt{\xi}}{2+\sqrt{\xi}} \right) - 2 \text{Li}_2 \left(\frac{2+\sqrt{\xi}}{4} \right) \right. \\
&\quad \left. - \frac{1}{6}\pi^2 + \ln^2 2 + \text{Li}_2 \left(\frac{2\sqrt{\xi}}{(2+\sqrt{\xi})(1+w)} \right) + \text{Li}_2 \left(\frac{2\sqrt{\xi}}{(2+\sqrt{\xi})(1-w)} \right) \right. \\
&\quad \left. + \text{Li}_2 \left((2+\sqrt{\xi}) \frac{(1+w)}{4} \right) + \text{Li}_2 \left((2+\sqrt{\xi}) \frac{(1-w)}{4} \right) \right] + 1 - \sqrt{\xi}, \quad (\text{A13})
\end{aligned}$$

$$\begin{aligned}
T_{10} &= \int \frac{dy dz}{\{(1-y)^2 - \xi\}^{3/2}} \frac{y^3}{z^2} \\
&= 2 \frac{(1-\sqrt{\xi})^2}{\xi^{3/2}} \left[-\ln \varepsilon + \frac{1}{2} \ln \xi - \ln(1+\sqrt{\xi}) + \ln(1-\sqrt{\xi}) + \ln 2 \right] \\
&\quad + \frac{8}{\xi} \left[\frac{1}{2} \ln \xi - \ln(1+\sqrt{\xi}) + \ln 2 \right] + \frac{4}{\xi} (1-\sqrt{\xi}). \quad (\text{A14})
\end{aligned}$$

We have used the short hand notation

$$w = \sqrt{\frac{1-\sqrt{\xi}}{1+\sqrt{\xi}}}.$$

References

- [1] J.H. Kühn, A. Reiter and P.M. Zerwas, Nucl. Phys. **B272** (1986) 560;
M. Anselmino, P. Kroll and B. Pire, Phys. Lett. **B167** (1986) 113
- [2] R.H. Dalitz and G.R. Goldstein, Phys. Rev. **D45** (1992) 1531;
W. Bernreuther, J.P. Ma and T. Schröder, Phys. Lett. **B297** (1992) 318;
W. Bernreuther, O. Nachtmann, P. Overmann and T. Schröder,
Nucl. Phys. **B388** (1992) 53; (E) Nucl. Phys. **B406** (1993) 516
- [3] F.E. Close, J.G. Körner, R.J.N. Phillips and D.J. Summers,
J. Phys. **G18** (1992) 1716
- [4] A.F. Falk and M.E. Peskin, Phys. Rev. **D49** (1994) 3320
- [5] J.G. Körner and M. Krämer, Phys. Lett. **B275** (1992) 495;
P. Bialas, J.G. Körner, M. Krämer and K. Zalewski, Z. Phys. **C57** (1993) 115
- [6] J.G. Körner, A. Pilaftsis and M.M. Tung, Z. Phys. **C63** (1994) 575
- [7] B. Falk and L.M. Sehgal, Phys. Lett. **B325** (1994) 509
- [8] T.D. Lee and M. Nauenberg, Phys. Rev. **133** (1964) 1549
- [9] J.G. Körner and D.H. Schiller, preprint DESY-81-043 (1981)
- [10] J.G. Körner and M.M. Tung, Z. Phys. **C64** (1994) 255
- [11] J. Jeršák, E. Laermann and P.M. Zerwas, Phys. Rev. **D25** (1982) 1218
- [12] J.G. Körner, G. Schuler, G. Kramer and B. Lampe, Z. Phys. **C32** (1986) 181;
J.G. Körner, D. Kreimer and K. Schilcher, Z. Phys. **C54** (1992) 503
- [13] S. Groote, J.G. Körner and M.M. Tung, to be published
- [14] G. Rodrigo and A. Santamaria, Phys. Lett. **B313** (1993) 441;
W. Bernreuther, preprint PITPA-94/31
- [15] M.M. Tung, preprint FTUV/94-4 (1994), Phys. Rev. **D52** no. 3 (in press)

Figure Captions

Fig. 1: Graphical representation of the $q\bar{q}g$ phase-space for massive quarks ($\xi = 4m_q^2/q^2 \neq 0$) in terms of the kinematic parameters $y = 1 - 2p_1 \cdot q/q^2$ and $z = 1 - 2p_2 \cdot q/q^2$. All boundary curves (shown are $\xi = 0.1, 0.2, \dots, 0.9$) intersect with the origin and have their maximum values on the axes at $y_+, z_+ = 1 - \sqrt{\xi}$.

Fig. 2: The c.m. energy dependence of (a) the longitudinal beam alignment polarization and (b) the total cross section for top-quark production at the one-loop QCD level. We have taken $m_t(m_t) = 174$ GeV and $\alpha_s^{(5)}(M_Z) = 0.123$.

Fig. 3: The longitudinal beam alignment polarization P_L^ℓ for $e^+e^- \rightarrow \gamma, Z \rightarrow t\bar{t}g$ as a function of the phase-space parameter $y = 1 - 2p_1 \cdot q/q^2$. The curves correspond to fixed c.m. energies of 350 GeV, 500 GeV and 1000 GeV.

Fig. 4: (a) Order α_s longitudinal beam alignment polarization and (b) total production rate for the bottom quark $m_b(m_b) = 4.3$ GeV as a function of the c.m. energy $\sqrt{q^2}$.

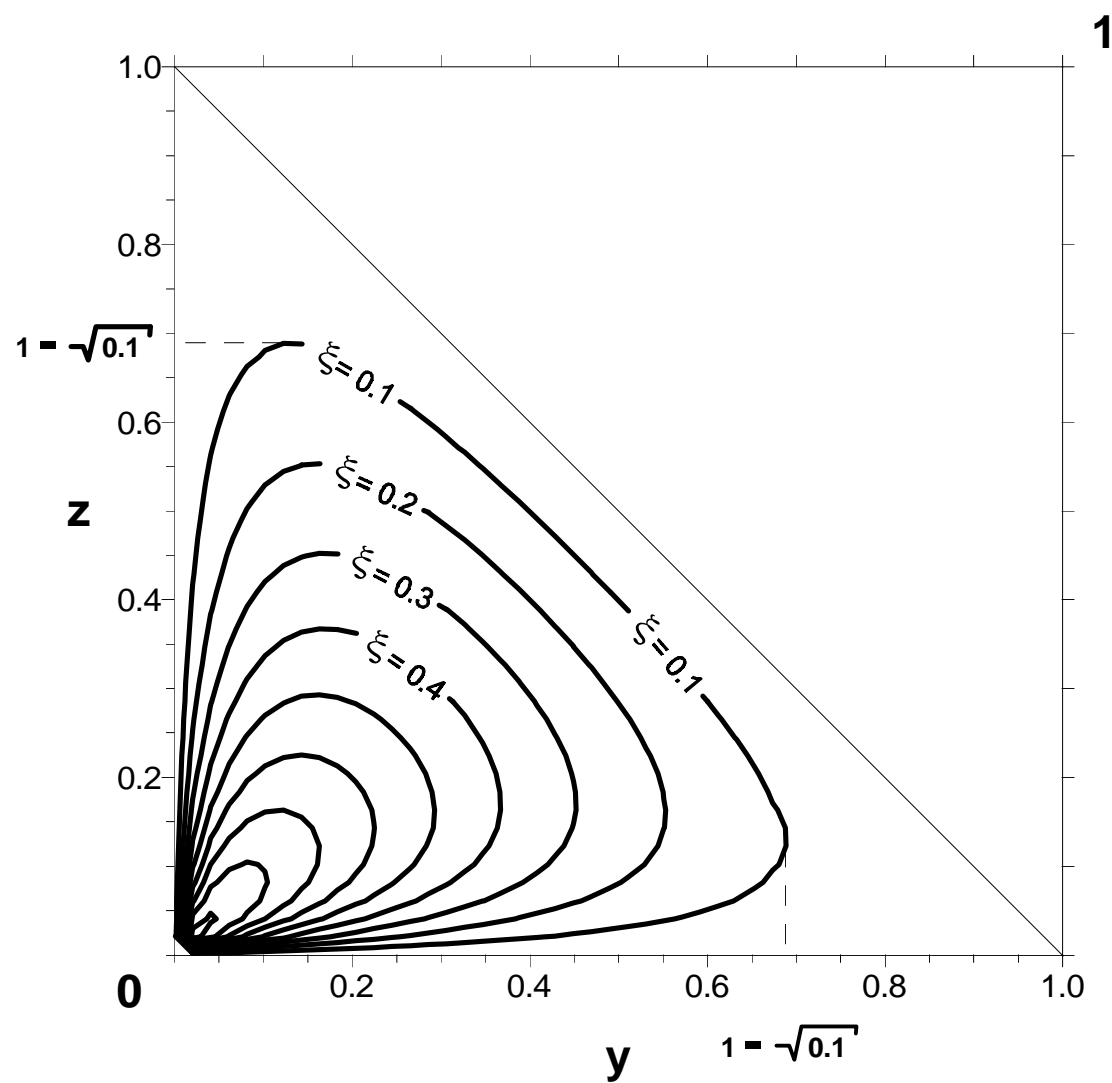


Figure 1

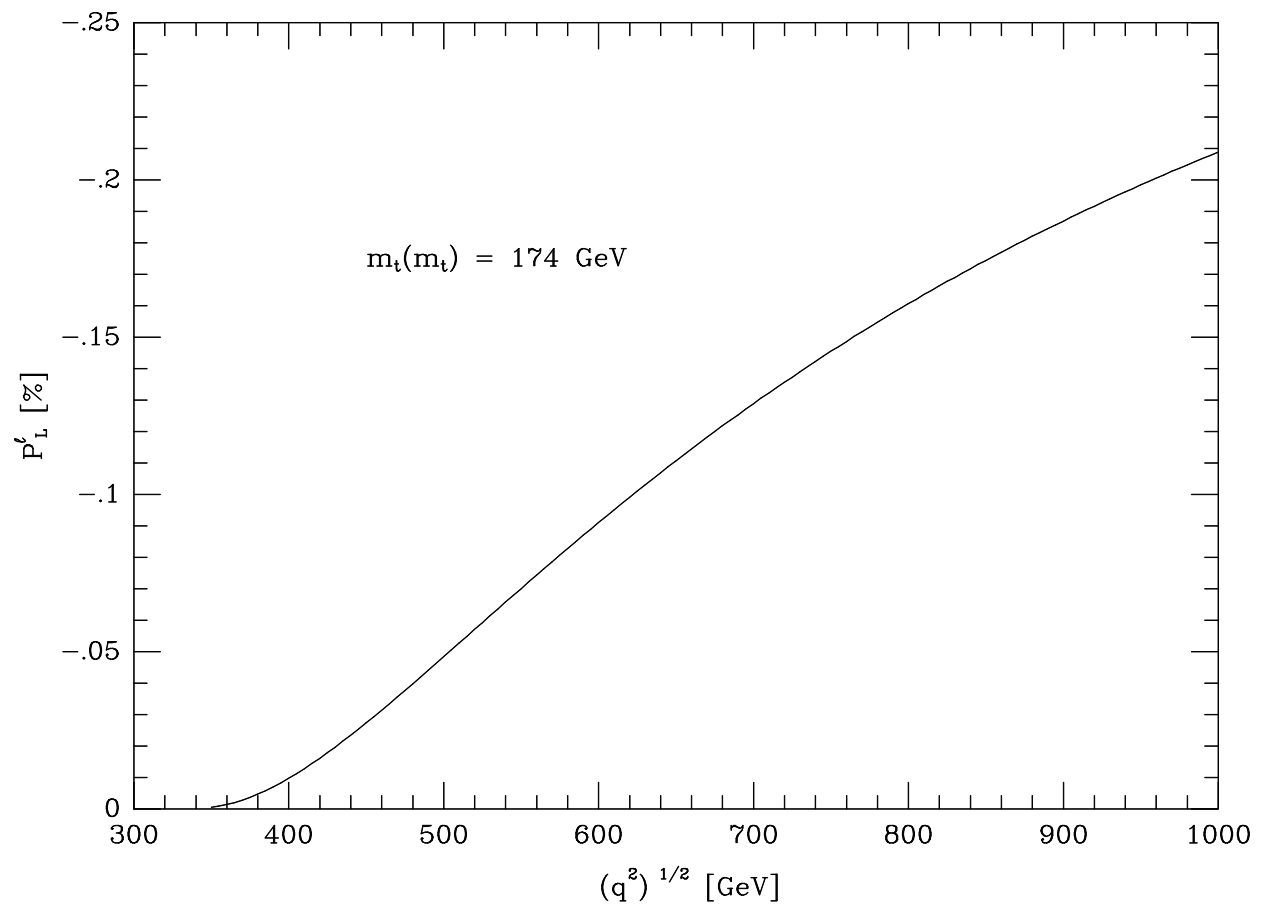


Figure 2(a)

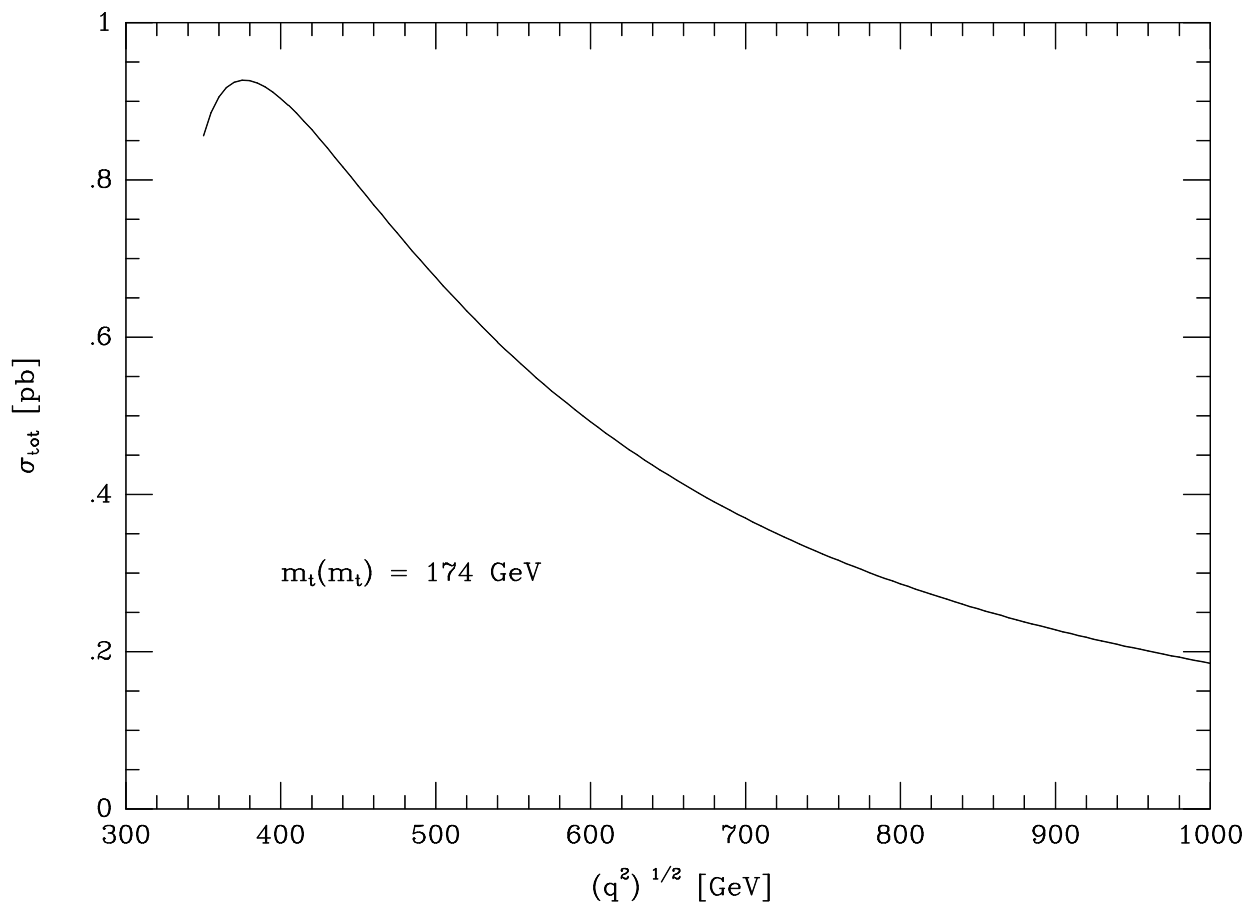


Figure 2(b)

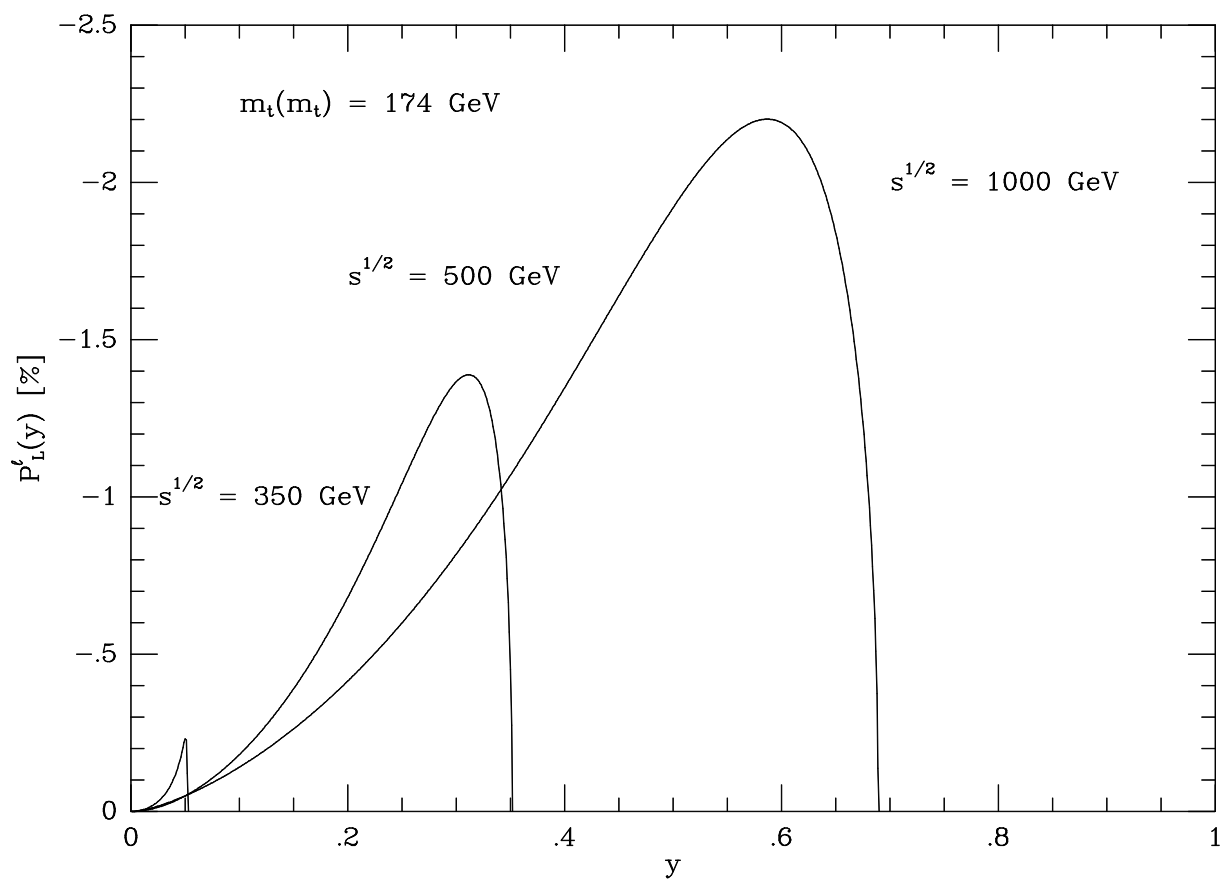


Figure 3

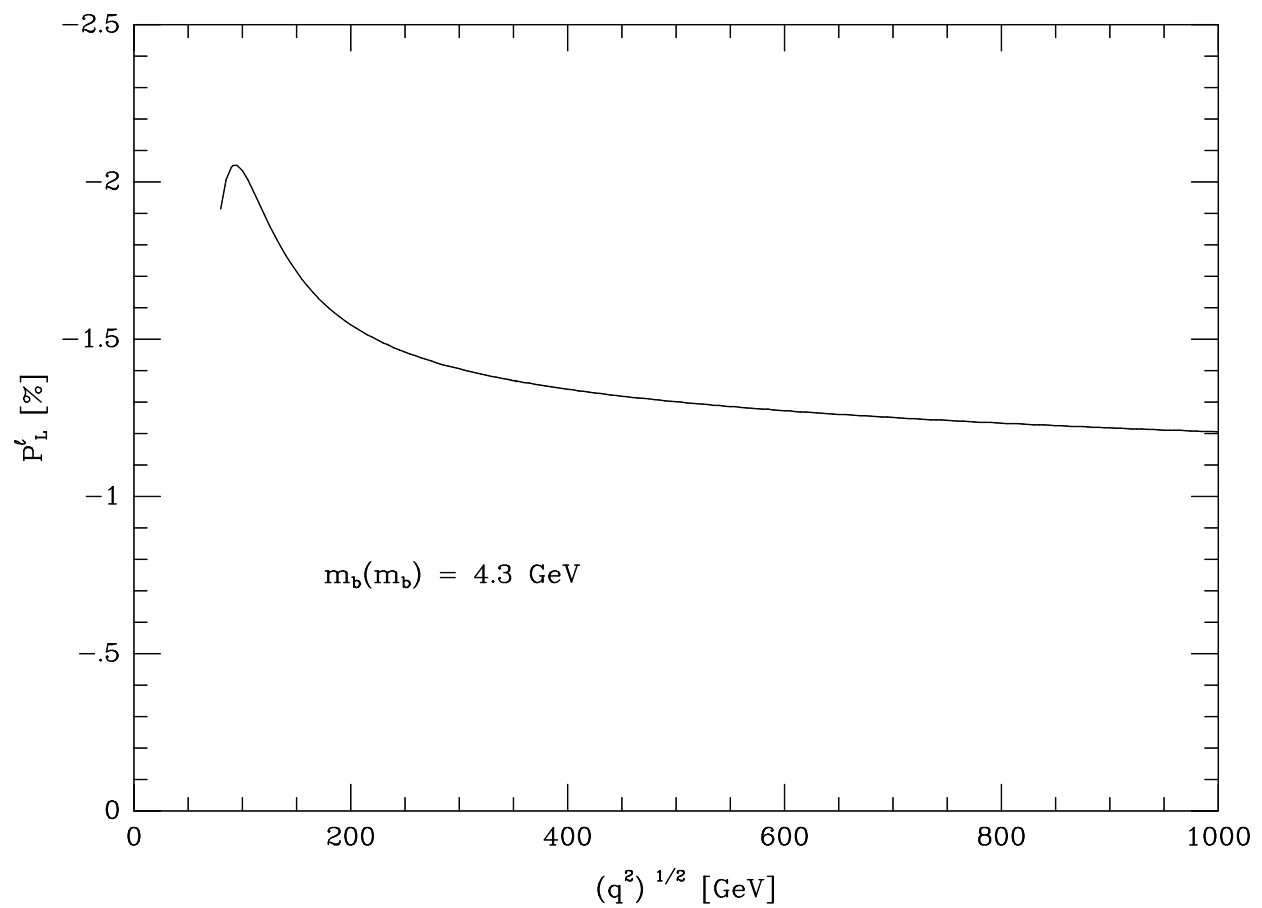


Figure 4(a)

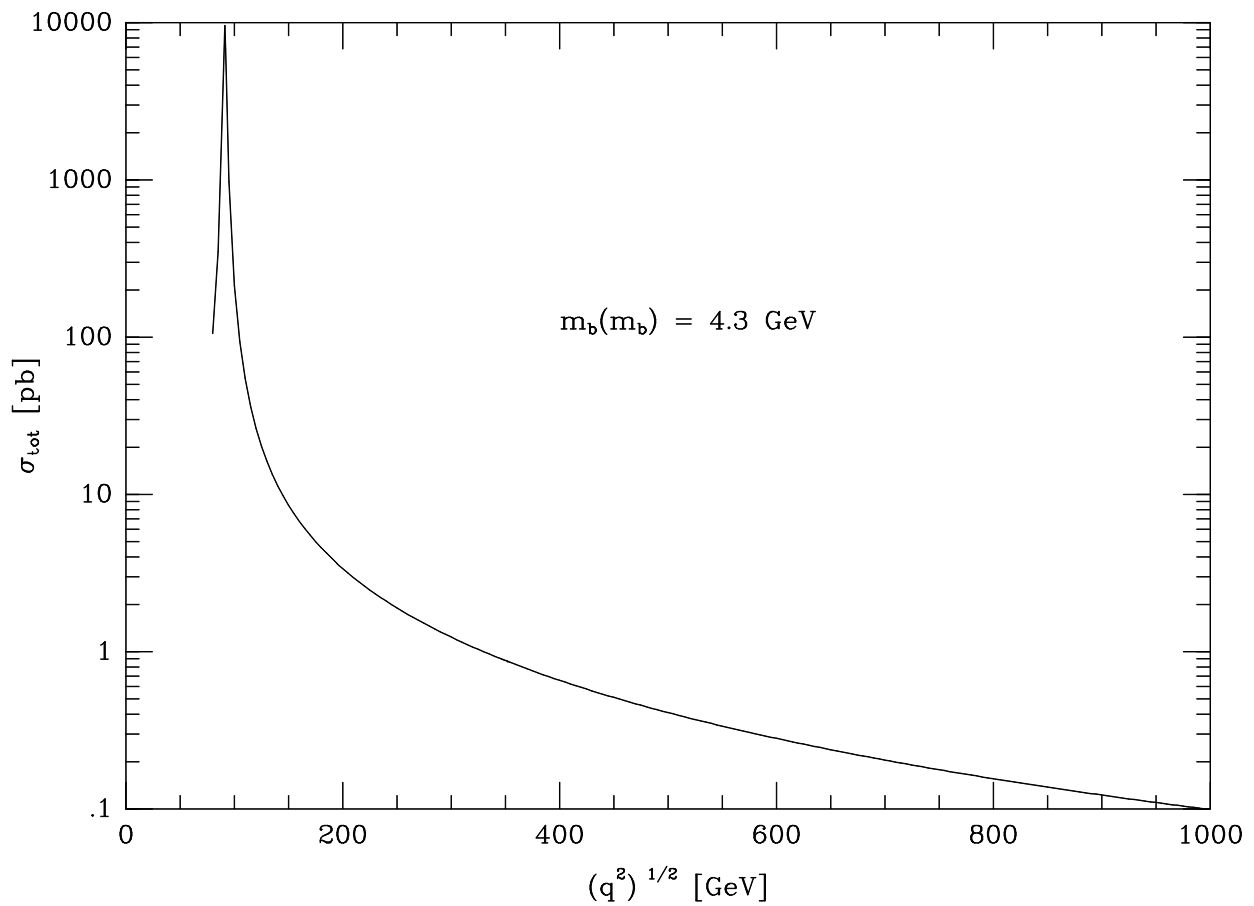


Figure 4(b)